SUPPLEMENTAL FIGURES AND LEGENDS

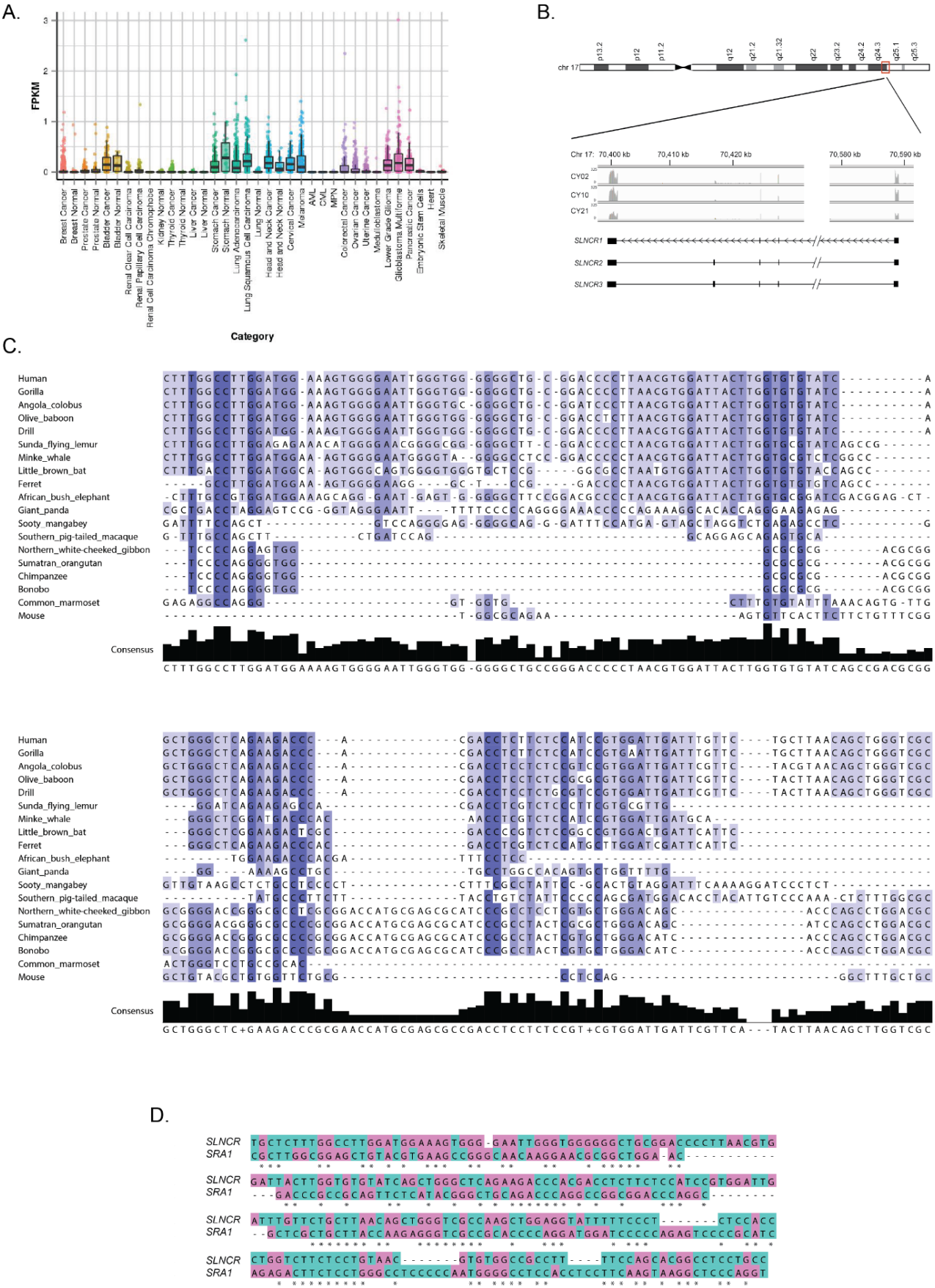

Figure S1: *SLNCR* is highly-conserved and expressed in multiple cancers, r**elated to Figure 1.** (A) MiTranscriptome expression data for *SLNCR* (linc00673) across all available cancer and normal tissue type cohorts. (B) Melanomas express three transcripts from

the *SLNCR* chromosomal 17 locus. Integrated Genome Viewer plot (middle) displaying melanoma RNA-seq read intensities corresponding to the indicated patient-derived melanomas. The three *SLNCR* isoforms are depicted below. (C and D) Alignments were performed using Clustal Omega and viewed in JALVIEW. (C) Alignment of *SLNCR* (nucleotides 462-572) with confirmed or predicted lncRNAs from the indicated species. Residues are shaded according to percent identity; dark blue >80%, blue >60%, light blue >40%. (D) Alignment of *SLNCR* (nucleotides 441-672) with *SRA1*. Purines are highlighted in pink, and pyrimidines are highlighted in teal. Asterisks denote identical nucleotides.

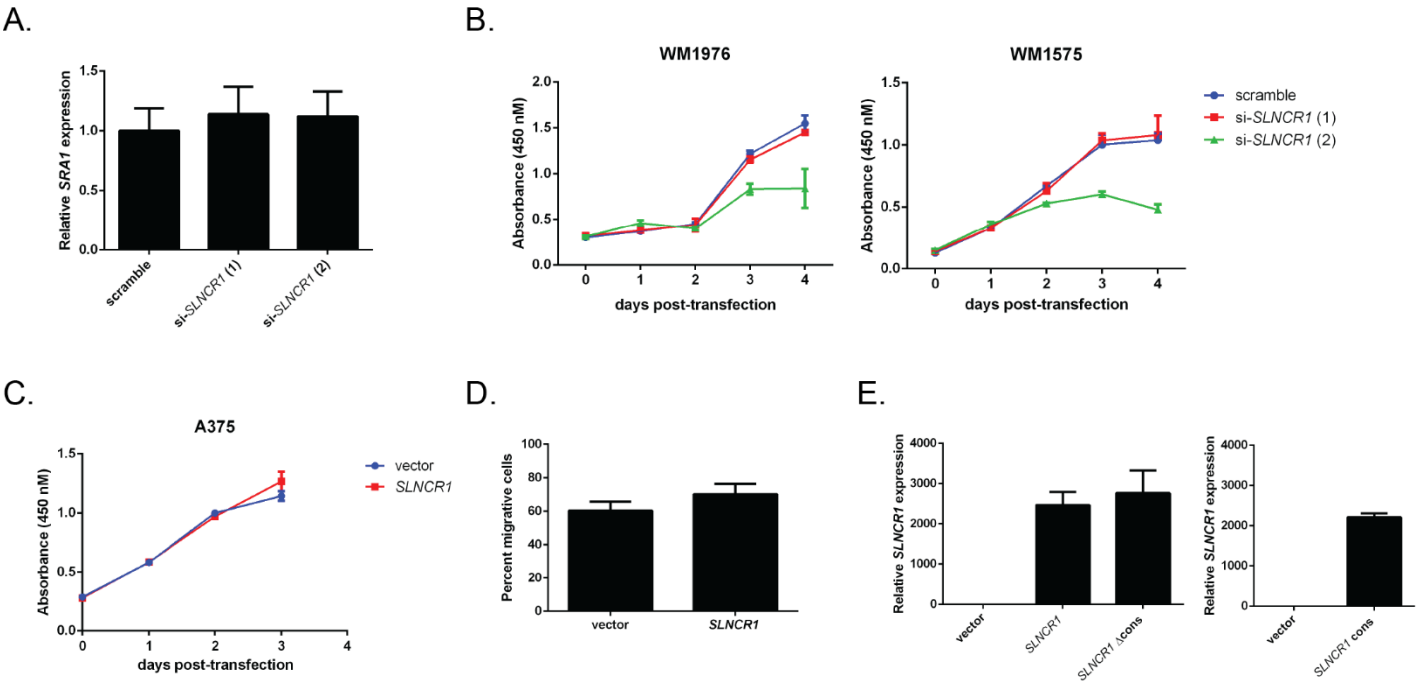

Figure S2: *SLNCR1* does not affect levels of *SRA1*, melanoma cell proliferation, viability or migration, related to Figure 2. (A) RT-qPCR of relative *SRA1* levels upon knockdown of *SLNCR1* in WM1976 melanoma cells. cDNA used is the same as shown in Figure 2A. (B) WM1976 (left panel) or WM1575 (right panel) melanoma short term cultures were transfected with the indicated siRNAs at Day 0, and proliferation was measured using WST-1 reagent every day for 4 days. The apparent decrease in cell proliferation observed with si-*SLNCR1* (2) is likely due to toxicity of the siRNA. (C) A375 cells were transfected with either an empty or *SLNCR1* expressing vector at Day 0, and proliferation was measured using WST-1 reagent every day for 3 days. (D) Transwell migration assays of A375 cells transfected with either an empty or *SLNCR1* expressing vector. Migration is calculated as the percent of migrating cells compared to total cells as counted in 8 fields of view. Shown is quantification from 3 independent replicates, represented as mean ± SD. (E) Relative *SLNCR1* expression in A375 cells transfected with the indicated plasmids. Quantification shown in the left panel was completed using a primer pair located outside of the conserved sequence, while the right panel used a primer pair located within the conserved sequence. Proliferation assays were repeated three times, and one representative assay is shown as mean ± SD. RT-qPCR data is represented as the fold change compared to A375 transfected with either scramble (A) or vector (E) control, normalized to *GAPDH*. Error bars represent standard deviations calculated from 3 reactions.

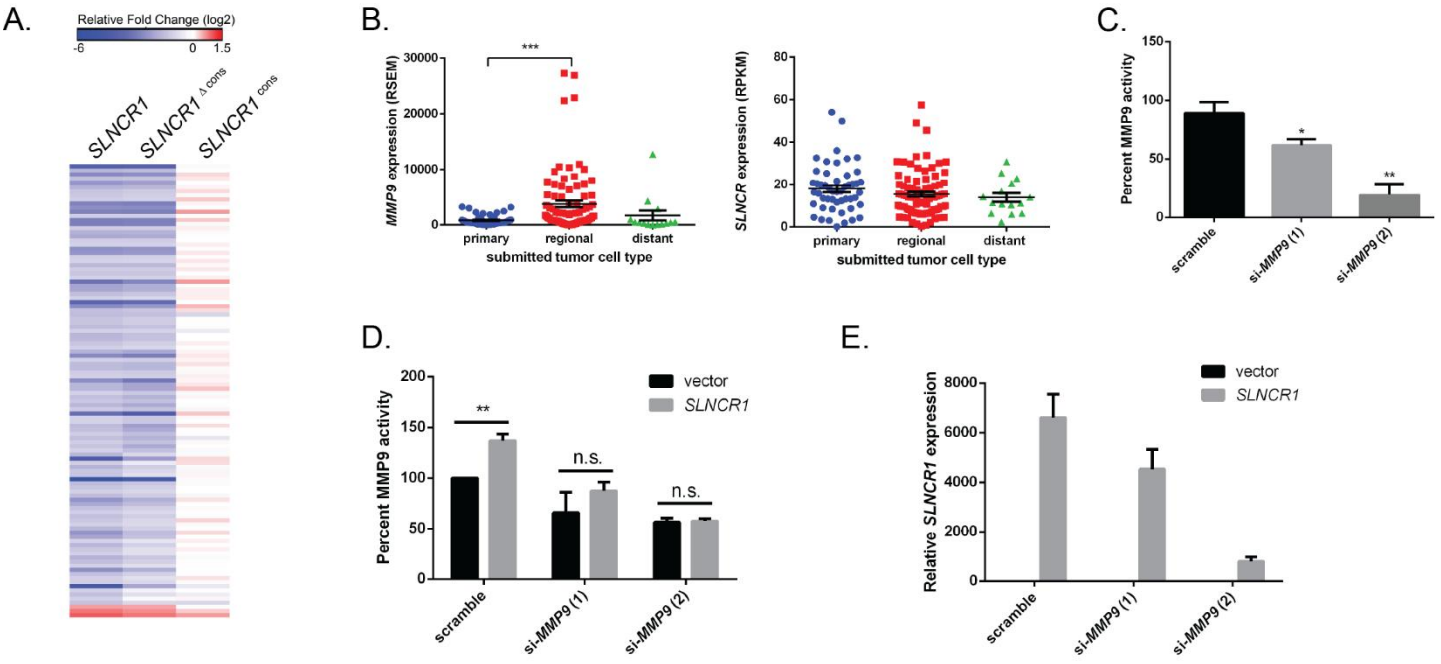

Figure S3: *SLNCR1* increases melanoma invasion through transcriptional upregulation of MMP9, related to Figure 3. (A) Heat map representing the log2 fold change of transcripts from A375 cells expressing *SLNCR1*, *SLNCR1*^{cons} or *SLNCR1*$^{\Delta cons}$, as compared to a vector only control. Shown are transcripts significantly regulated by *SLNCR1* (adjusted p-value < 0.05, fold change >2). (B) Box plot of *MMP9* expression (left panel) and *SLNCR* (right panel) from 150 TCGA, categorized by the tumor cell type submitted for sequencing. Primary = primary tumor, regional = regional metastasis, and distant = distant metastasis. Data are represented as mean ± SEM. (C and D) As described in Figure 3 (C-E). (C) Quantification of three independent zymograms of cell supernatants from A375 cells transfected with the indicated siRNAs. (D). Quantification of three independent zymograms of cell supernatants from A375 cells transfected with the indicated siRNAs (E) Relative *SLNCR1* expression in A375 cells transfected with the indicated plasmids and siRNAs. RT-qPCR data is represented as the fold change compared to A375 transfected with a vector and scramble control, normalized to *GAPDH*. Error bars represent standard deviations calculated from 3 reactions. Significance was calculated using the Student's t-test: * p-value < 0.05, ** p-value < 0.005, *** p-value < 0.0005, ns = not significant.

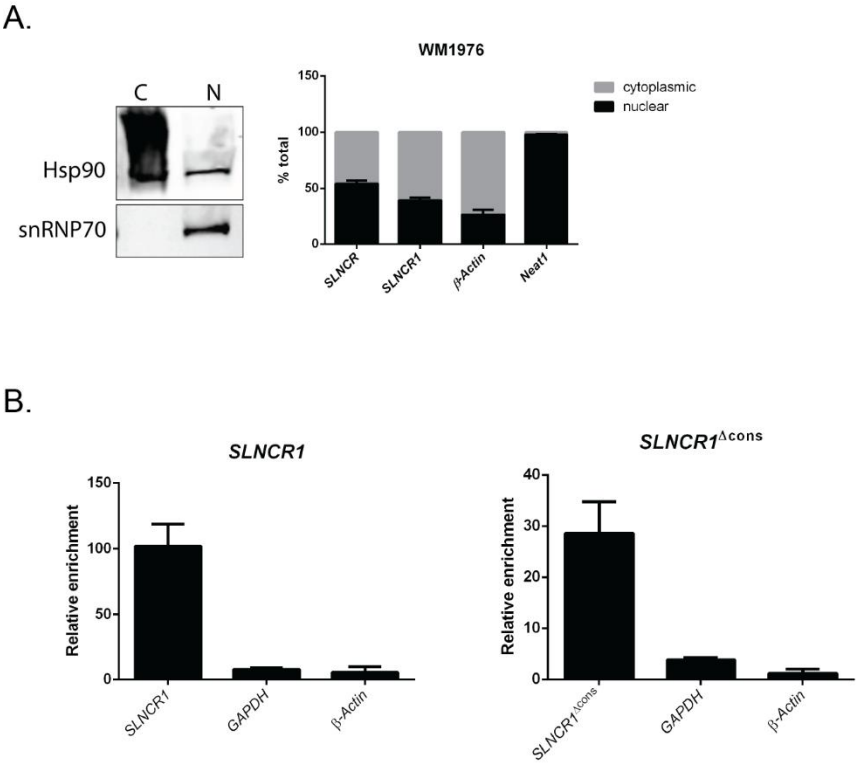

Figure S4: MS2-based IP of the nuclear fraction of *SLNCR1*, related to Figure 4. (A) Fractionation of the melanoma short term culture WM1976 reveals that *SLNCR1* is located in both the cytoplasm and nucleus. Left: western blot of cytoplasmic (C) and nuclear (N) fractions of WM1976. The blot was probed with α-Hsp90 and α-snRNP70 antibodies to confirm successful fractionation. Right: RT-qPCR of cytoplasmic and nuclear RNAs from the fractionation shown at left. *SLNCR* localization was determined with primers that amplify all *SLNCR* isoforms, while *SLNCR1* localization was determined with *SLNCR1* isoform-specific primers. Cytoplasmic enrichment of *β-Actin* mRNA and nuclear enrichment of the *NEAT1* lncRNA confirms successful fractionation of RNA. (B) FLAG-tagged MS2 was immunoprecipitated from A375 cells transfected with plasmids expressing FLAG-tagged MS2 and the indicated *SLNCR1* construct, compared to control cells expressing *SLNCR1* without encoded MS2 stem loop structures. Relative enrichment of the indicated transcripts as measured by RT-qPCR compared to RNA enriched from cells expressing *SLNCR1* without MS2 stem loops. Total proteins and RNAs were released by incubating in Laemmli buffer at 95°C for 5 minutes.

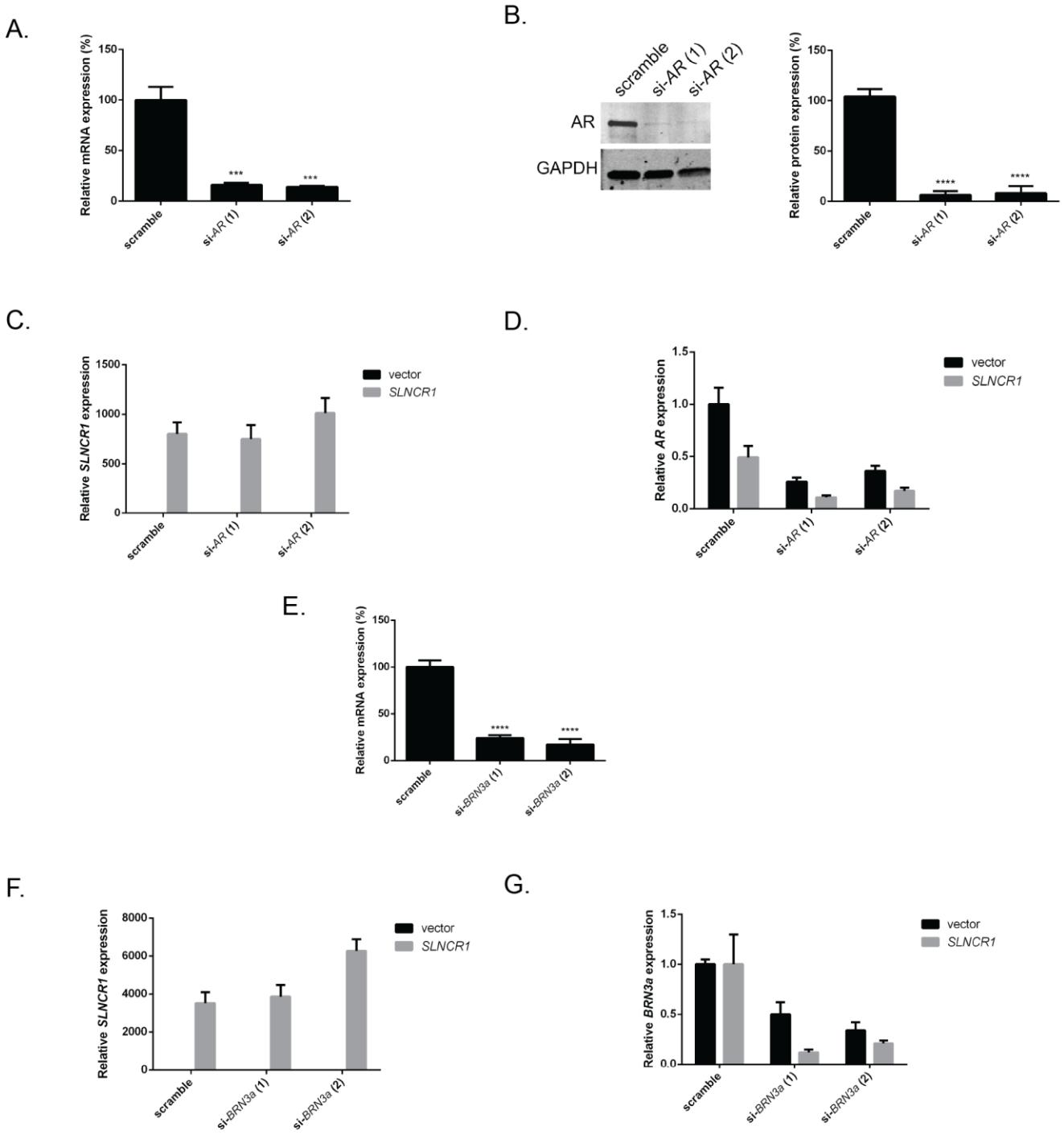

Figure S5: Knockdown of AR or Brn3a does not affect *SLNCR1* overexpression, related to Figure 5. (A) Relative *AR* expression in A375 cells transfected with the indicated siRNAs. (B) Western blot of A375 cell lysates following transfection with the indicated siRNAs. Left panel: representative blot probed with α-AR and α-GAPDH antibodies. Right panel: quantification from three independent replicates, normalized to GAPDH. (C) Relative *SLNCR* expression in A375 cells co-transfected with the indicated plasmids and siRNAs. (D) Same as in (C), but for relative *AR* expression. (E) Relative *Brn3a* expression in A375 cells transfected with the indicated siRNAs. (F) Relative *SLNCR* expression in A375 cells co-transfected with the indicated plasmids and siRNAs. (G) Same as in (F), but for relative *BRN3a* expression. All RT-qPCR represent the fold change compared to scramble or vector/scramble controls after normalization to *GAPDH*. Error bars represent standard deviations calculated from 3 reactions. Significance was calculated using the Student's t-test: *** p-value < 0.0005, **** p-value < 0.0001.

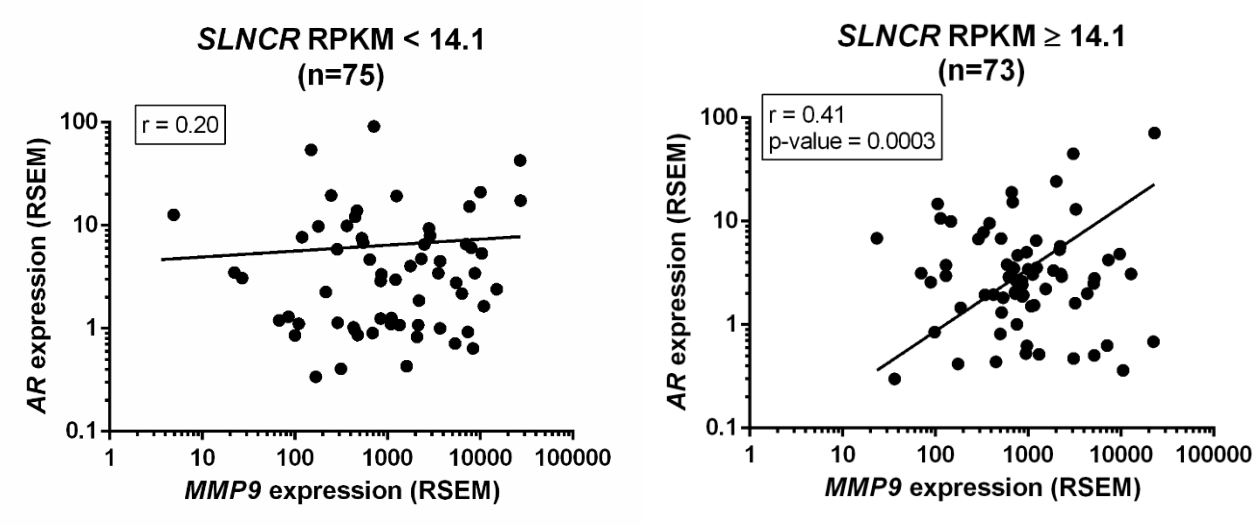

Figure S6: *AR* and *MMP9* expression is significantly correlated in high-*SLNCR* expressing melanomas, related to Figure 6. Scatterplots of *AR* and *MMP9* expression from TCGA patient melanomas expression low (RPKM < 14.1, left panel) or high (RPKM ≥ 14.1, right panel) *SLNCR*. Pearson correlation coefficient (r) and significance are shown.

A.

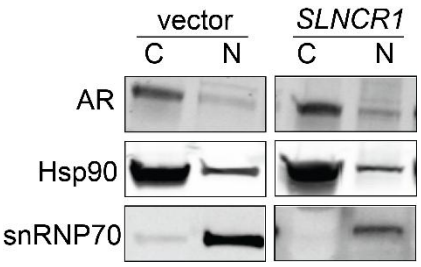

B.

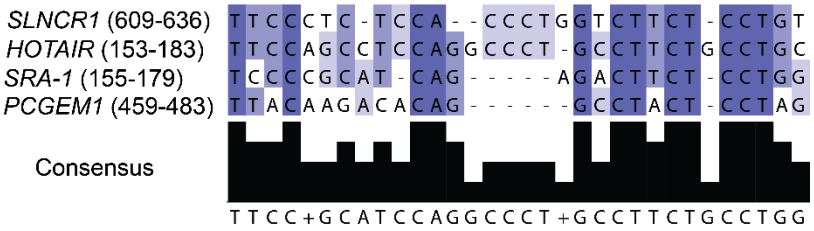

Figure S7: *SLNCR1* does not affect localization of AR and contains a region similar to other AR-associated lncRNAs, related to Figure 7. (A) Western blot of cytoplasmic (C) and nuclear (N) fractions of A375 cells transfected with an empty or *SLNCR1*-expressing vector. The blot was probed with α-Hsp90 and α-snRNP70 antibodies to confirm successful fractionation, and localization of AR was determined using an α-AR antibody. (B) Alignment of AR-bound regions of *SLNCR1*, *HOTAIR*, *PCGEM1* and a similar region of *SRA1*. Alignment was performed as in Figures S1C and S1D. Numbers in parentheses indicate the lncRNA nucleotides shown in the alignment.

SUPPLEMENTAL TABLES

Supplemental tables available as downloadable excel spreadsheets:

Table S1: Expression of lncRNAs in patient-derived melanomas, related to Figure 1. RNA-Seq reads were mapped to the BROADs Human Body Map lincRNA catalog, and FPKMs for each indicated samples are listed. Included are lncRNAs expressed at >1 FPKM in all 4 primary melanomas. *SLNCR1* is highlighted in red. (Excel File: Table S1)

Table S4: Differential expression of transcripts upon siRNA knockdown of *SLNCR1* in WM1976, related to Figure 2. Sheet 2 contains expression of all transcripts. Sheet 3 contains transcripts significantly regulated by knockdown of *SLNCR1* (adjusted p-value < 0.05, fold change >2). Genes in the AR transcriptional network (as defined by MetaCore analysis) are highlighted in red. (Excel File: Table S4)

Table S5: Differential expression of transcripts upon expression of *SLNCR1* constructs in A375, related to Figure 3. Sheet 2 contains differential expression of transcripts upon expression of *SLNCR1*. Sheet 3 contains differential expression of transcripts upon expression of $SLNCR1^{\Delta cons}$. Sheet 4 contains differential expression of transcripts upon expression of $SLNCR1^{cons}$. (Excel File: Table S5)

Cancer Type	Amplified Region	Q-value	Overall Frequency of Amplification
Melanoma	Chr17:41471733-78605474	0.242	49.5%
Lung NSC	Chr17:55353997-78605474	0.128	39.6%
All lung	Chr17:55353997-78605474	0.0949	39.9%
Ovarian	Chr17:47316963-78605474	0.12	30.1%

Table S2: *SLNCR* is located on a chromosomal region commonly amplified in melanoma, lung and ovarian cancers, related to Figure 1. Data is taken from Broad's TCGA Tumorscapes (Beroukhim et al., 2010).

Cells	Gender	Age	Notes
A375	Female	54	Metastatic melanoma
WM1575	Male	No data	Melanoma
WM1862	No data	No data	Primary/Radial Growth Phase
WM1976	No data	No data	Melanoma
WM3228	No data	No data	Melanoma
WM3670	No data	No data	Metastasis
CY02	Male	40	Stage IV melanoma
CY10	Male	29	Stage III melanoma
CY21	Female	66	Stage IV melanoma

Table S3: Melanoma cell lines used in this study, related to Figure 1. 'WM' cells are from Dr. Meenhard Herlyn's collection at the Wistar Institute, 'CY' melanomas were isolated by Dr. Charles Yoon, Brigham and Woman's Hospital, Boston, MA

Sequence	Name	Type
AAGAGGATGGGAAGGACTGAT	si-*SLNCR1* (1)	siRNA
CTGATGGGAAGGACTGATCCA	si-*SLNCR1* (2)	siRNA
ACGGCTTGCCCTGGTGCAGTA	si-*MMP9* (1)	siRNA
AACCTTTGAGGGCGACCTCAA	si-*MMP9* (2)	siRNA
AAGGAACTCGATCGATCGATCATT	si-*AR* (1)	siRNA
CTGCTACTCTTCAGCAGCATTATT	si-*AR* (2)	siRNA
TCGGATTTGGAGTGTCCGTTA	si-*BRN3a* (1)	siRNA
CGCCACGATGATGATGTCCATGAA	si-*BRN3a* (2)	siRNA
GAGAACGTGGTGGAATCAGA	*SLNCR* Forward (all isoforms)	qPCR
TCCCATCCTCTTTCTTGTCC	*SLNCR* Reverse (all isoforms)	qPCR
GGACCCCTTAACGTGGATTAC	*SLNCR1* conserved Forward	qPCR
AAATACCTCCAGCTTGGCG	*SLNCR1* conserved Reverse	qPCR
GAAAGAGGATGGGAAGGACTG	*SLNCR1* Forward	qPCR
ATCAAATCCAGAGCTCCTGC	*SLNCR1* Reverse	qPCR
TGGAACAGGCATTGGAAGAC	*SRA1* Forward	qPCR
TTGCACCAGTAGAGCCATTC	*SRA1* Reverse	qPCR
CGAACTTTGACAGCGACAAG	*MMP9* Forward	qPCR
CACTGAGGAATGATCTAAGCCC	*MMP9* Reverse	qPCR
GGTTACACCAAAGGGCTAGAA	*AR* Forward	qPCR
GACTTGTAGAGAGACAGGGTAGA	*AR* Reverse	qPCR
CTTTCGGAGTGTTTGTGGATATAC	*BRN3a* Forward	qPCR
GACGGGTACTTGTGCTCAG	*BRN3a* Reverse	qPCR
ACAGAGTCACCAGTTTTCCG	*NEAT1* Forward	qPCR
ACTTGATAACACCCACACCC	*NEAT1* Reverse	qPCR
GAAGGTGAAGGTCGGAGT	*GAPDH* Forward	qPCR
GAAGATGGTGATGGGATTTC	*GAPDH* Reverse	qPCR
AACTTCTACAATGAGCTGCG	*B-ACTIN* Forward	qPCR
CCTGGATAGCAACGTACATGG	*B-ACTIN* Reverse	qPCR

Table S6: siRNA and oligo sequences used in this study, related to Figures 1-6.

SUPPLEMENTAL EXPERIMENTAL PROCEDURES

RNA-sequencing and bioinformatics

For MSTC RNA-seq, cDNA libraries were prepared from 1ug of total RNA using the Illumina TruSeq RNA sample preparation kit (v2). Libraries were pooled and sequenced on the Illumina HiSeq 2000 platform. Normalized read counts (FPKM) were generated in Cufflinks v2.1.1 (http://cole-trapnell-lab.github.io/cufflinks/) by mapping onto the hg19 build of the human transcriptome (http://support.illumina.com/sequencing/sequencing_software/igenome.html). For RNA-Seq of *SLNCR1* depleted or over-expressing cells, library preparation and analysis was performed by The Center for Cancer Computational Biology, Dana-Farber Cancer Institute, Boston, MA. Two independent replicate of all conditions were sequenced. RNA was selected using NEBNext® PolyA mRNA Magnetic Isolation Module and libraries were prepared using NEBNext® Ultra™ RNA Library Prep Kit for Illumina®. Libraries were sequenced on Illumina® NextSeq 500 platform with Paired End 75bp sequencing. Sequencing reads were aligned to the Human Reference Genome (assembly hg19) using RNA-specific STAR aligner (Dobin et al., 2013), and quality was assessed using the Broad Institutes's RNA-SeQC tool (DeLuca et al., 2012). Read-counts were counted using featureCounts tool (Liao et al., 2014). All normalizations and differential expression analysis was performed using the DESeq software suite (Anders and Huber, 2010). Heat maps were generated with Gene-E software (http://www.broadinstitute.org/cancer/software/GENE-E/).

SLNCR homologs were identified through BLAST of the *SLNCR* sequence against the Reference RNA sequence database (blast.ncbi.nlm.nih.gov). Alignments were performed in Clustal Omega (Goujon et al., 2010; Sievers et al., 2011), and viewed in Jalview (Waterhouse et al., 2009). BAM files from RNA-seq of melanomas was visualized using the Integrated Genome Viewer (broadinstitute.org/igv/) (Robinson et al., 2011; Thorvaldsdottir et al., 2013).

For TCGA analyses, raw FASTQ files were obtained for 150 randomly selected sub-cutaneous melanoma samples following dbGaP approval using the GeneTorrent software for CGHub (Wilks et al., 2014). The *SLNCR1* consensus transcript was aligned to each FASTQ using Bowtie2 (Langmead and Salzberg, 2012). RPKM values were calculated for cross-sample comparisons. Expression of mRNAs was accessed through the Broad Institute TCGA Genome Data Analysis Center (Harvard, 2015).

Small interfering RNAs

All siRNAs were purchased from Qiagen. *SLNCR1* specific siRNA sequences were custom synthesized and used at a final concentration of 10nM. MMP-9-targeting siRNAs were used at a final concentration of 7.5 nM, AR-targeting siRNAs at 10 nM, and Brn3a-targeting siRNAs at 5 nM.

Gelatin Zymography

Gelatin zymography was performed as previously described, with slight modifications (Toth and Fridman, 2001). Cells were seeded at a density of 25 x 10^4 cells per well in 6-well dishes, and transfected with the indicated plasmids and/or siRNAs 24 hours later. Cells were washed with PBS and transitioned to 900 µl of serum free media 24 hours post-transfection. Supernatant was removed 24 hours later and non-adherent cells were pelleted by centrifugation at 300 x g for 5 minutes at 4°C. The remaining supernatant was then concentrated 5-fold using Millipore Amicon Ultra 10kDa cutoff centrifugal devices. Samples were incubated at room temperature for 10 minutes in SDS sample buffer without a reducing agent, and then electrophoresed on 10% Criterion™ Zymogram Gel (Bio-Rad). After electrophoresis, gels were washed briefly in dH_2O, followed by 2 40 minute washes in 1x renaturation buffer (Bio-Rad); incubated for 18 hours at 37°C in 1x development buffer (Bio-Rad); and stained with 0.1% Coomassie brilliant blue R250. Ratios of MMP9 compared to MMP2 were quantified by ImageJ software densitometric analysis of the 92-kd and 72-kd proteolytic bands, which correspond to MMP9 and MMP2, respectively.

Migration and Invasion Assays

Twenty-four hours post seeding at 25 x 10^4 cells in a 6-well plate, cells were transfected with either 2,500 ng of the indicated plasmid or the indicated siRNAs. For migration and invasion assays using A375 cells, 2.5 x 10^4 cells in serum-free media were plated in either BD BioCoat™ matrigel inserts or uncoated control inserts (Corning), placed into DMEM with 30% FBS (fetal bovine serum), and incubated for 16 hours. For the melanoma short term cultures, 10 x10^4 or 7.5 x10^4 cells, for WM1976 or WM1575, respectively, in serum-free media were seeded in the chambers, placed into DMEM with 30% FBS (fetal bovine serum), and incubated for 22 hours. Cells that did not migrate or invade were removed using a cotton tipped swap, chambers were rinsed twice with PBS, and stained using Fisher HealthCare™ PROTOCOL™ Hema 3™ Fixative and Solutions. Cells were imaged on 20x magnification in 8 fields of view for 3 independent replicates.

RIP assays

For AR RIP, HEK293T cells were seeded in a 10 cm dish, and 24 hours later were co-transfected with 15 µg pEGFP-C1-AR and 10 µg of *SLNCR1*- or *SLNCR1*$^{\Delta cons}$- or *SLNCR1*$^{\Delta 568\text{-}637}$- expressing plasmids. For Brn3a RIP, HEK293T cells were seeded in a 10cm dish, and co-transfected with 15 µg pCDNA-Brn3a and 10 µg of *SLNCR1*- or *SLNCR1*$^{\Delta cons}$- expressing plasmids. For UV-crosslinking of Brn3a IPs, cells were washed in PBS, and UV-crosslinked in a UV-Stratalinker at 400 mJ/cm^2 in 5 mls of ice cold PBS. For both AR and Brn3a IPs, cells were lysed for 10 minutes in IP lysis buffer (20 mM Tris pH 7.4, 10 mM NaCl, 2 mM EDTA, supplemented with 0.5% Triton-X-100, RNaseOUT (Invitrogen), 1 mM PMSF, and cOmplete Protease Inhibitor Cocktail (Roche), NaCl was added to a final concentration of 300 mM and incubated on ice for an additional 10 minutes, and spun at 18,000 x g for 10 minutes at 4°C. Lysate was split and immunoprecipitated with 1.5 µg α-AR antibody or IgG negative control, or 1 µg α-Brn3a antibody or IgG negative control, rotating for 18 hours at 4°C. Lysate was incubated with Protein A Dynabeads® (Life Technologies) (25 µl slurry) for 1 hour at 4°C, followed by 4 x 0.5 ml washes in wash buffer (50 mM Tris pH 7.4, 500 mM NaCl, supplemented with 0.05% Triton-X-

100). For non-crosslinked cells, beads were boiled in 2x Laemmli buffer for 5 minutes are 95°C, and bound fractions were split for protein and RNA analysis. For UV-crosslinked cells, beads were resuspended in wash buffer and split for protein and RNA analysis. For RNA, 100 µg of proteinase K was added in proteinase K digestion buffer (300 mM NaCl, 200 mM Tris pH 7.5, 25 mM EDTA, 2% SDS), and incubated at 65°C for 30 minutes with gentle mixing.

SUPPLEMENTAL REFERENCES

Anders, S., and Huber, W. (2010). Differential expression analysis for sequence count data. Genome biology *11*, R106.

Beroukhim, R., Mermel, C.H., Porter, D., Wei, G., Raychaudhuri, S., Donovan, J., Barretina, J., Boehm, J.S., Dobson, J., Urashima, M., *et al.* (2010). The landscape of somatic copy-number alteration across human cancers. Nature *463*, 899-905.

DeLuca, D.S., Levin, J.Z., Sivachenko, A., Fennell, T., Nazaire, M.D., Williams, C., Reich, M., Winckler, W., and Getz, G. (2012). RNA-SeQC: RNA-seq metrics for quality control and process optimization. Bioinformatics *28*, 1530-1532.

Dobin, A., Davis, C.A., Schlesinger, F., Drenkow, J., Zaleski, C., Jha, S., Batut, P., Chaisson, M., and Gingeras, T.R. (2013). STAR: ultrafast universal RNA-seq aligner. Bioinformatics *29*, 15-21.

Goujon, M., McWilliam, H., Li, W., Valentin, F., Squizzato, S., Paern, J., and Lopez, R. (2010). A new bioinformatics analysis tools framework at EMBL-EBI. Nucleic acids research *38*, W695-699.

Harvard, B.I.o.M.a. (2015). Broad Institute TCGA Genome Data Analysis Center: Firehose.

Langmead, B., and Salzberg, S.L. (2012). Fast gapped-read alignment with Bowtie 2. Nature methods *9*, 357-359.

Liao, Y., Smyth, G.K., and Shi, W. (2014). featureCounts: an efficient general purpose program for assigning sequence reads to genomic features. Bioinformatics *30*, 923-930.

Robinson, J.T., Thorvaldsdottir, H., Winckler, W., Guttman, M., Lander, E.S., Getz, G., and Mesirov, J.P. (2011). Integrative genomics viewer. Nature biotechnology *29*, 24-26.

Sievers, F., Wilm, A., Dineen, D., Gibson, T.J., Karplus, K., Li, W., Lopez, R., McWilliam, H., Remmert, M., Soding, J., *et al.* (2011). Fast, scalable generation of high-quality protein multiple sequence alignments using Clustal Omega. Molecular systems biology *7*, 539.

Thorvaldsdottir, H., Robinson, J.T., and Mesirov, J.P. (2013). Integrative Genomics Viewer (IGV): high-performance genomics data visualization and exploration. Briefings in bioinformatics *14*, 178-192.

Toth, M., and Fridman, R. (2001). Assessment of Gelatinases (MMP-2 and MMP-9 by Gelatin Zymography. Methods Mol Med *57*, 163-174.

Waterhouse, A.M., Procter, J.B., Martin, D.M., Clamp, M., and Barton, G.J. (2009). Jalview Version 2--a multiple sequence alignment editor and analysis workbench. Bioinformatics *25*, 1189-1191.

Wilks, C., Cline, M.S., Weiler, E., Diehkans, M., Craft, B., Martin, C., Murphy, D., Pierce, H., Black, J., Nelson, D., *et al.* (2014). The Cancer Genomics Hub (CGHub): overcoming cancer through the power of torrential data. Database : the journal of biological databases and curation *2014*.